

Study on Quaternary Ammonium Modified Tentacle-Type Cellulose Beads and Its Adsorption for $\text{Ag}(\text{CN})_2^-$

Na Zhang, Cheng-Xianyi Zhou, Tong-Hui Xie, Yong-Kui Zhang

Department of Pharmaceutical and Biological Engineering, School of Chemical Engineering, Sichuan University, Chengdu 610065, People's Republic of China

Correspondence to: Y.-K. Zhang (E-mail: zhangyongkui@scu.edu.cn)

ABSTRACT: A novel anion exchange resin based on cellulose has been prepared to adsorb $\text{Ag}(\text{CN})_2^-$ for the urgent demand of silver and the high toxicity of metal-cyanide complexes. Quaternary ammonium groups were grafted onto cellulose beads as main active sites in tentacle-type through a series of chemical reactions. The substitution degree of each reaction was determined to be about 0.854, 2.125, and 2.899 mmol g^{-1} , respectively. The resin exhibited excellent spherical shape with microporous structure by the observation of optical microscopy and scanning electron microscope. Moreover, the adsorption experiments demonstrated the adsorption was fast in alkaline condition. Fitting the data into isotherm and kinetic models gave the conclusion that the adsorption behavior matched better with Langmuir model and pseudo-second-order kinetic in initial time followed pseudo-first-order kinetic model in later phase. The equilibrium adsorption capacity was determined to be 3.016 mmol g^{-1} . With the advantages of high capacity, short equilibrium time, and alkaline resistance, the resin would be considered to a top-priority adsorbent for the separation of $\text{Ag}(\text{CN})_2^-$. © 2014 Wiley Periodicals, Inc. *J. Appl. Polym. Sci.* **2014**, *131*, 40987.

KEYWORDS: adsorption; cellulose and other wood products; resins; separation techniques

Received 31 December 2013; accepted 7 May 2014

DOI: 10.1002/app.40987

INTRODUCTION

With the shortage of resource and the aggravation of heavy metal pollution, great effort has been directed to the recovery of heavy metal from aqueous solution. The heavy metal is present in water in variety forms, including salts and various metal complexes. $\text{Ag}(\text{CN})_2^-$ is considered as the main form of silver when it is extracted from ores and silver wastes by cyanidation.^{1,2} The $\text{Ag}(\text{CN})_2^-$ needs to be recovered from leachate as much as possible because of the urgent demand of silver and the high toxicity of metal-cyanide complexes. What is noteworthy is that the dissociation of metal-cyanide complexes can release more toxic substance (HCN) when under acidic condition or being exposed directly to ultraviolet light.^{3–5} Moreover, the best leaching rate was obtained when the pH value of lixivium was around 11. Therefore, the metal-cyanide leach streams usually stay in the pH range of 10–12 in industries.^{6,7} Given that, it is of great urgency to search suitable method for $\text{Ag}(\text{CN})_2^-$ recovery in alkaline condition.

Among available methods developed for heavy metal removal, ion exchange has attracted great attention because it possessed the advantages in affinity, regeneration, and loading capacity.^{3,7–9} However, the practical application of this method has been limited due to its high cost of preparation and operation.¹⁰

To reduce the cost, many efforts have been made to develop novel ion exchange resins which process low manufacture cost or good adsorption performance. The study of ion exchange used in cyanidation mainly focuses on searching suitable resins for the sorption of gold from cyanide leaching solution. The recently reported resins have exhibited excellent characters such as high capacity, rapid adsorption, and alkaline resistance; however, it is difficult to possess all these qualities meanwhile for these adsorbents.^{3,10–13} In addition, particular study on the sorption of $\text{Ag}(\text{CN})_2^-$ ion onto ion exchange resin in cyanidation is relatively few.¹¹ Therefore, it is necessary to develop a novel ion exchange resin for $\text{Ag}(\text{CN})_2^-$ adsorption, which can possess the valuable properties mentioned above as much as possible.

Cellulose is the most abundant and renewable biopolymer in nature which has numerous advantages in application.¹⁴ Besides the large surface area, the abundant hydroxyl groups on it indicate its enormous potential in modification, making it economically feasible to be applied in the field of wastewater treatment and chemical area.

As for the modification of cellulose, grafting tentacle-type ligands might be a viable option to create a novel resin which possesses both low-cost and high adsorption capacity.^{6,15} The amount of activated sites on support, which can be offered by

modified ligands, have a big influence on the adsorption capacity of ion exchange resin. Therefore, grafting tentacle-type ligands instead of monolayer ones allows the possibility of multilayer adsorption, leading to a high adsorption capacity, especially for small molecules like $\text{Ag}(\text{CN})_2^-$ ions.^{15–17} Moreover, in theory, the outstretched spacer arm can reach and contact the adsorbate easily, which may result in a fast adsorption. Therefore, grafting tentacle-type ligands on suitable support might be a feasible approach.

In order to obtain a good performance for $\text{Ag}(\text{CN})_2^-$ adsorption in alkaline condition, strong base anion exchange resin can be taken into consideration, some authors have reported that strong base resins could load dicyanide complexes more better than any other species.¹⁰ Therefore, there is an attempt to synthesize a novel strong base anion exchange resin for $\text{Ag}(\text{CN})_2^-$ sorption, and quaternary ammonium groups which have been widespread used in strong base anion exchange resins were chosen as the active sites.^{18,19}

In this article, a novel strong anion exchange resin based on cellulose, which possesses high capacity and short equilibrium time for $\text{Ag}(\text{CN})_2^-$ adsorption in alkaline condition, was created through three substitution reactions. The cellulose was prepared into spherical beads by the modified water/oil emulsification, and then the epichlorohydrin (EPC), triethylenetetraamine (TATE), and glycidyltrimethyl ammonium chloride (GTA) were introduced onto cellulose beads successively to obtain a novel resin which functionalized with quaternary ammonium groups in tentacle-type. The substitution degree of each reaction was calculated and analyzed in detail. In addition, Fourier transform infrared (FTIR) spectroscopy, laser particle size analyzer, optical microscopy (OM), and scanning electron microscopy (SEM) were used in combination to carry out a structure measurement of the resin. The adsorption performance of the resin for $\text{Ag}(\text{CN})_2^-$ adsorption was carefully studied under various conditions including pH, phase contact time, and initial concentration. Furthermore, the isotherm and kinetic parameters were investigated in detail.

EXPERIMENTAL

Materials

Degreasing cotton was provided by Runhua (Guangdong, China). GTA was purchased from Dongying Guofeng Fine Chemical Co. (Shandong, China). Other reagents, including sorbitantriolate (Span 85), transformer oil, carbon disulfide (CS_2), hydroxide sodium (NaOH), sodium carbonate (Na_2CO_3), dimethyl sulfoxide (DMSO), EPC, and TATE were of analytical grade from Kelong (Sichuan, China).

Methods

Preparation of Cellulose Beads. Cellulose beads were prepared using a double emulsification procedure as shown in Figure 1.²⁰ First, the degreasing cotton was soaked in NaOH solution to get alkali cellulose, which was more reactive. Then, the alkali cellulose was kept for aging for several days to obtain low degree of polymerization (DP) alkali cellulose. After that, the low DP cellulose was reacted with CS_2 to produce cellulose xanthate, which was then diluted with NaOH solution to get

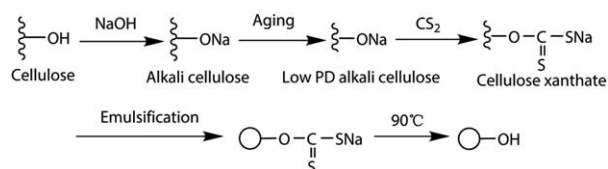


Figure 1. Preparation route of cellulose beads.

viscose suspension. Next, the viscose suspension was emulsified with an oil phase until it uniformly dispersed in sphere shape. The emulsion was then heated to 90°C and kept for hours to solidify the spherical structure by the reason of reduction of cellulose xanthate to cellulose at high temperatures. Subsequently, dropping of mixture temperature followed by centrifugation can obtain the spherical cellulose. Finally, these beads were washed with deionized water and screened out with standard sieves.

Synthesis of Cellulose 1, Cellulose 2, and Cellulose 3. The tentacle-type anion exchange resin was prepared in three steps. First, 5 g of wet cellulose beads were poured into a mixture of 2.5 mL of EPC, 10 mL of 1 mol L^{-1} NaOH solution, and 10 mL of DMSO. The suspension was incubated in a thermostatic water bath at 40°C for 2.5 h to synthesize epoxy cellulose beads (cellulose 1). Then, the cellulose 1 were reacted with a mixture of 5 mL of TETA, 10 mL of 1 mol L^{-1} Na_2CO_3 solution, and 45 mL deionized water at 60°C for 12 h to synthesize aminated cellulose beads (cellulose 2). Third, the quaternized cellulose beads (cellulose 3) were achieved by suspending cellulose 2 in the mixture of 20 g of GTA, 25 mL of DMSO, and 25 mL of deionized water. The suspension was stirred at 60°C for 6 h. At the end of each step, the synthesized compound was separated by filtration, rinsed with deionized water until the residual reactant was completely eliminated. The cellulose 3 was also need to be regenerated with NaCl solution followed by washing with deionized water to make sure all the resins were in chloride form. The products of the three steps were dried under oven at 60°C for 12 h and stored in a desiccator.

Characterization

Substitution Degrees. The substitution degree of each reaction was determined successively. The substitution degree of step 1 was obtained by measuring the quantity of introduced epoxy group in cellulose 1 according to the method of National Standard of China.^{20,21} In this work, 0.2 g dried beads of cellulose 1 was treated with a 25 mL mixture of hydrochloric acid and acetone for 0.5 h. The mixed solution was titrated with 0.15 mol L^{-1} NaOH solution after separating. The epoxy value was calculated according to eq. (1):

$$C_{\text{epoxy}} = \frac{C_{\text{NaOH}} \times (V_{\text{NaOH}} - V_{\text{NaOH}}^*)}{m_1} \quad (1)$$

The substitution degree of step 2 was obtained by measuring the quantity of basic functional groups introduced in cellulose 2 according to the method of retro-titration.²² For this purpose, 0.1 g dried beads of cellulose 2 was treated with 100 mL of 0.01 mol L^{-1} HCl solution for 1 h. Then, the solution was titrated with 0.01 mol L^{-1} NaOH solution after separation. The concentration of amine groups was calculated according to eq. (2):

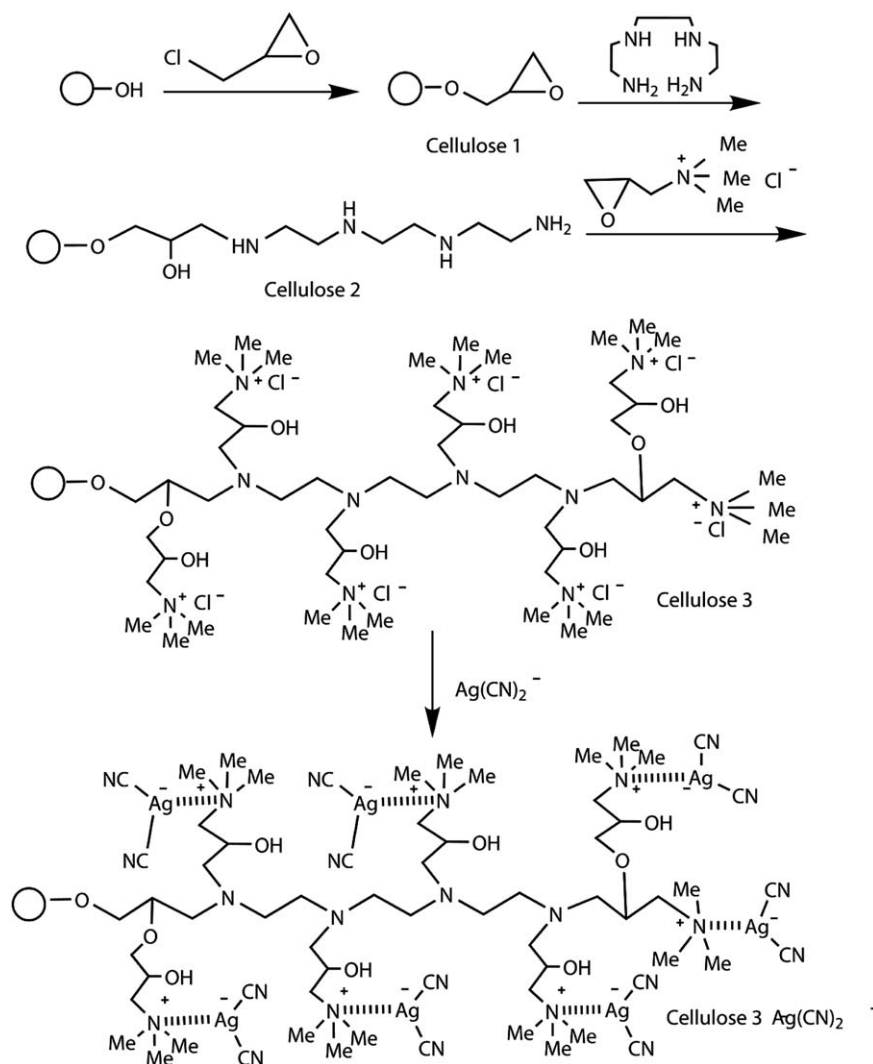


Figure 2. Synthesis routes used to prepare cellulose 1, cellulose 2, and cellulose 3, and adsorption of $\text{Ag}(\text{CN})_2^-$ on cellulose 3.

$$C_{\text{NH}_2} = \frac{C_{\text{NaOH}} \times (V_{\text{NaOH}} - V_{\text{NaOH}}^*)}{m_2} \quad (2)$$

The substitution degree of step 3 was obtained by measuring the exchange capacity of cellulose 3 according to the method of AgNO_3 titration.²³ For this, 0.1 g dried beads of cellulose 3 were packed into a 300 mm \times 19 mm exchange column and washed by 100 mL of 0.5 mol L⁻¹ Na_2SO_4 adequately. The effluent was titrated with 0.02 mol L⁻¹ AgNO_3 solution. The concentration of ammonium groups was calculated according to eq. (3):

$$C_{-\text{NH}_3^+} = \frac{C_{\text{AgNO}_3} \times (V_{\text{AgNO}_3} - V_{\text{AgNO}_3}^*)}{m_3} \quad (3)$$

where C_{NaOH} is the concentration of NaOH solution (mol L⁻¹), V_{NaOH} and V_{NaOH}^* are the volumes of NaOH solution spent in the titration of nonreacted acid's excess (mL) of blank sample and test sample respectively, C_{AgNO_3} is the concentration of AgNO_3 solution (mol L⁻¹), V_{AgNO_3} and $V_{\text{AgNO}_3}^*$ are the volumes of AgNO_3 solution (mL) of blank sample and test sample,

respectively, m_1 , m_2 , and m_3 are the weight of cellulose 1, cellulose 2, and cellulose 3 (g), respectively.

Water Retention. A total of 1.0 g dried beads of cellulose 3 were immersed in 40 mL of distilled water for 24 h, and then the beads were centrifuged at 4000 rpm for 20 min to determine the water retention capacity, which can be expressed according to eq. (4):

$$W = \frac{V}{m_3} \quad (4)$$

where V is the volume of wet cellulose 3 (mL).

FTIR Analysis. Samples were prepared by mixing 1 mg of material with 100 mg of spectroscopy grade KBr. The FTIR spectra were recorded using Nicolet 6700 equipment with detector at 4 cm⁻¹ resolution from 400 to 4000 cm⁻¹ and 32 scans per sample.

Particle Size Measurement. Particle size distribution of cellulose 3 was measured by using a laser diffraction particle size

Table I. Concentration of Epoxy, Amine, and Ammonium Groups

Material	C _{epoxy} (mmol g ⁻¹)	C _{NH-NH₂} (mmol g ⁻¹)	C _{-NH₃⁺} (mmol g ⁻¹)
Cellulose 1	0.854	-	-
Cellulose 2	-	2.125	-
Cellulose 3	-	-	2.899

analyzer (Rise-2002, Jinan). Quadruplicate measurements were made and mean particle size was measured.

OM and SEM. OM image of cellulose 3 was recorded on a Nikon ECLIPSE E600 microscope. SEM was performed with a JSM-7500F microscope.

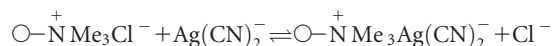
Adsorption Experiment

Adsorption was determined by the batch method. The parameters considered for study were pH, contact time and initial concentration of adsorbate. The pH of the solution was adjusted by adding 0.1 mol L⁻¹ NaOH or 0.1 mol L⁻¹ HCl. For kinetic and isotherm studies, a series of 50 mL stoppered conical flasks were filled with 20 mL Ag(CN)₂⁻ solution of varying concentrations (0.044–44.5 mmol L⁻¹), maintained at the desired temperature and pH. The flasks were agitated in an orbital shaker at 170 rpm and taken out at a given time interval successively from 0.1 min to 480 min. The samples were separated by filtration and the concentration of remaining Ag(CN)₂⁻ in the filtrate were detected by atomic absorption spectrophotometry (AAS).²⁴ A SpectrAA 220FS AAS was used with the following conditions: lamp, silver hollow cathode; source current, 7 mA; wavelength, 328.1 nm; slitwidth, 0.2 nm; burner, a nonluminous air-acetylene flame being used throughout, with acetylene flow 2.9 L min⁻¹ and air flow 13.5 L min⁻¹.

RESULTS AND DISCUSSION

Characterization of Cellulose 1, Cellulose 2, and Cellulose 3

Synthesis routes of celluloses 1, 2, 3 and sorption of Ag(CN)₂⁻ on cellulose 3 were illustrated in Figure 2. As shown, the functional group of cellulose 3 is quaternary amine, and chloride ions are adsorbed to the ammonium groups through electrostatic interactions. In the process of adsorption, the Ag(CN)₂⁻ ions are adsorbed on the resin while chloride ions are released to the solution, which is shown here:^{3,11,25}



The results of the concentration of epoxy, amine, and quaternary ammonium groups were presented in Table I. And these

Table II. Comparison of Water Retention on Different Adsorbents

Adsorbent	Water retention (mL g ⁻¹)	References
AV-17-10P	4.6	19
AN-85-10P	3.8	19
AN-25	3.9	19
SBAE	5.7	23
Amberlite IRA-400	3.7	23
Cellulose 3	5.9	In this study

results indicated the success of the synthesis methodology applied in this work.

The cellulose beads were activated with EPC by reaction between hydroxyl group of cellulose and chlorine of EPC, the epoxy value of cellulose 1 was 0.854 mmol g⁻¹. The epoxy groups in cellulose 1 were used to anchor TETA with cellulose matrix to get aminated derivatives, the concentration of amine was 2.125 mmol g⁻¹.

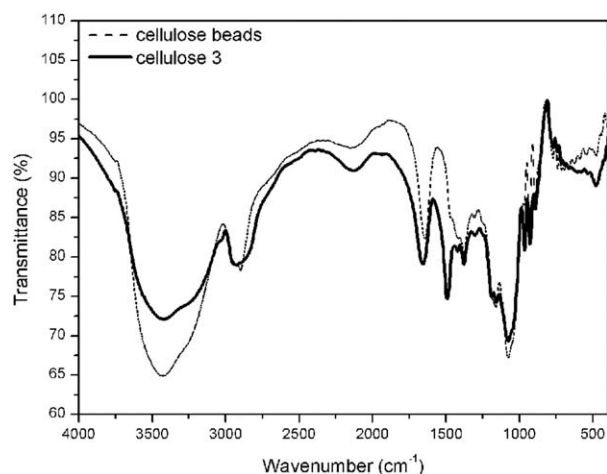
In addition to improve the density of function groups, EPC and TETA also served as crosslinking agent to withstand the tension (repulsion charges) caused by the introduction of GTA.^{26,27}

The strong base anion exchange resin (cellulose 3) was eventually obtained by functionalizing cellulose 2 with quaternary ammonium groups, and the degree of quaternization was 2.899 mmol g⁻¹. There were three main factors contribute to the high value. First of all, the design of tentacle-type ligands could offer a large amount of reaction sites (amine group) for GTA, improving the density of function groups significantly. Second, GTA can react with hydroxyl group as well as amine group as shown in Figure 2, leading to a higher degree of quaternization than amination.²⁸ In general, epoxy group is liable to react with amine group rather than hydroxyl group because of the stronger nucleophilicity of amine group. This explained why hydroxyl groups were not chosen as the main reaction sites for epoxy groups, although it was abundant on cellulose. Third, not only cellulose beads but also fixed EPC and GTA could offer hydroxyl group, which can be further modified as shown in Figure 2. All these made the resin possible to possess a high density of function groups by fixing EPC, TETA, and GTA on the cellulose beads.

From the data presented in Table II, the cellulose-based anion exchange resin exhibited a better water retention capacity than some full-synthesized ion exchange resins, the high strong hydrophilic of cellulose 3 made the resin more suitable to be used in aqueous solution.

FTIR Characterization

The chemical construction of cellulose 3 was characterized by FTIR spectroscopy. For illustration, the FTIR spectra of

**Figure 3.** FTIR spectra of cellulose beads and cellulose 3.

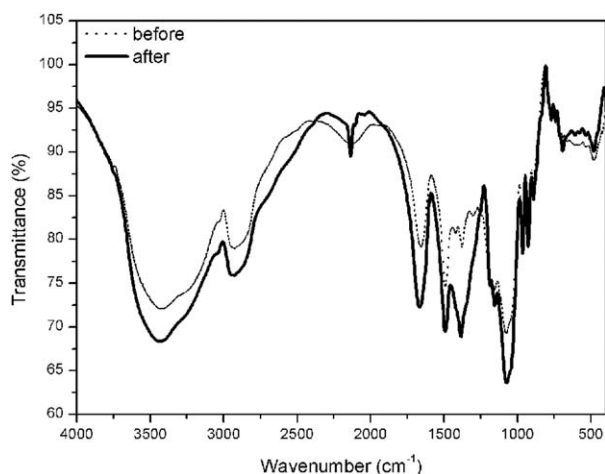


Figure 4. FTIR spectra of cellulose 3 before and after adsorption.

unmodified cellulose beads and cellulose 3 were shown in Figures 3 and 4 showed the FTIR spectra of cellulose 3 before and after adsorption.

As depicted in Figure 3, the band located at 3426 cm^{-1} in cellulose beads is attributed to —OH stretching vibration. But in cellulose 3, the band in the area of $3100\text{—}3600\text{ cm}^{-1}$ becomes broad because of the stretching vibration of N—H in —NH_x and the existence of $\text{—CH}_2\text{—N}^+(\text{CH}_3)_3$ moiety.²⁹ The stretching vibration of C—H in both —CH_3 and $\text{—CH}_2\text{—NH—CH}_2\text{—}$ also makes the band located at 2924 cm^{-1} become broad. The other relevant changes observed in the FTIR spectra of cellulose bead in relation to cellulose 3 are the appearances of band at 3021,

1491 , 1421 , 1190 , and 964 cm^{-1} . The band at 3021 cm^{-1} corresponds to deformation vibration of C—H in epoxy group. The bands at 1491 and 1190 cm^{-1} correspond to C—N vibration of $\text{—N}^+(\text{CH}_3)_3\text{Cl}^-$.³⁰ The bands at 1421 and 1378 cm^{-1} correspond to symmetric deformation vibration of —C—H in $\text{—N}^+(\text{CH}_3)_3$.³¹ And the band at 964 cm^{-1} corresponds to $\text{—CH}_2\text{—N}^+(\text{CH}_3)_3$.

As shown in Figure 4, the main difference between the two spectra is the appearance of sharp bands at 2135 and 2099 cm^{-1} , which is the characteristic peaks of $\text{—C}\equiv\text{N}$ in $\text{Ag}(\text{CN})_2^-$.^{32,33} The appearance of these bands indicated the success of the adsorption of $\text{Ag}(\text{CN})_2^-$.

Surface Morphology

Figure 5(A,B) showed the external morphology and volume change of cellulose 3 before and after drying by the observation of OM and SEM. Clearly, the samples exhibited excellent spherical shape both in water and dry state with an average diameter of about 90 and $40\text{ }\mu\text{m}$, respectively. The perfect spherical shape would benefit the adsorbent with suitable fluid dynamics for metal ions adsorption. The average diameter of wet beads was confirmed by the result of laser particle size analyzer, which was measured as $84.60\text{ }\mu\text{m}$. The big difference of volumes between wet and dried beads indicated the cellulose beads might exhibit a good water retention, which would benefit the application of the ion exchange resin in aqueous solution.

Figure 5(C,D) showed the surface structure more clearly. As shown, the resin exhibited rough surface with micropores centered at about 20 nm . The surface roughness and pore

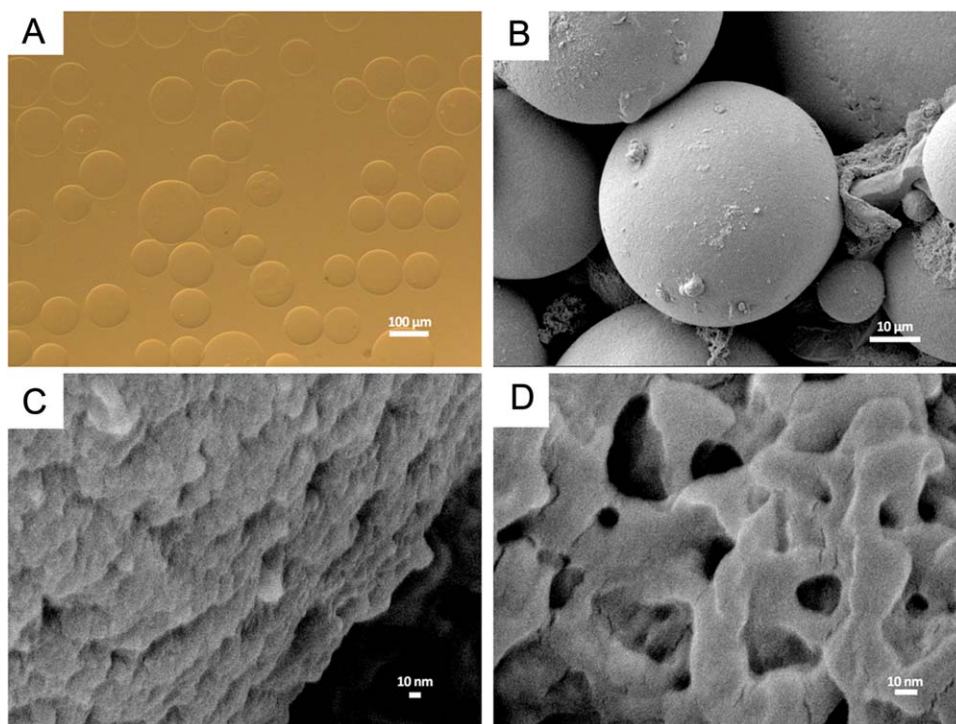


Figure 5. OM image of cellulose 3 before drying (A) and SEM images of cellulose 3 after drying (B–D). [Color figure can be viewed in the online issue, which is available at wileyonlinelibrary.com.]

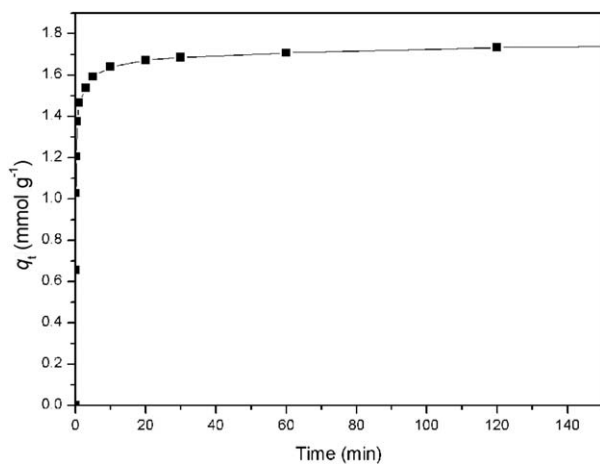


Figure 6. Effect of contact time on the adsorption of $\text{Ag}(\text{CN})_2^-$ onto cellulose 3. $[\text{Ag}(\text{CN})_2^-] = 6.68 \text{ mmol L}^{-1}$; temperature = 25°C ; pH = 11.0; amount of adsorbent = 20 mg; stirring rate = 200 rpm.

morphology of the beads could be a valuable property which may significantly increase the surface area for $\text{Ag}(\text{CN})_2^-$ binding.

Effect of Contact Time

The effect of contact time on the sorption of $\text{Ag}(\text{CN})_2^-$ on cellulose 3 was shown in Figure 6. As seen, the adsorption equilibrium of $\text{Ag}(\text{CN})_2^-$ attained in about 20 min which can be attributed to the equilibration of available adsorbing sites on the surface of the resin. In addition, the sorption increased sharply at beginning, about 88% of the ultimate adsorption occurred in the first 3 min, indicating the cellulose 3 possess a quite rapid sorption for $\text{Ag}(\text{CN})_2^-$. This deduction was proved by the comparison of adsorption time for metal-cyanide complexes on different adsorbents as shown in Table III. The rapid adsorption is promising by virtue of the economic viability because equilibrium time plays a major role in designing water treatment plants.^{35,36} Based on this result, the adsorption time was determined to be 20 min for the rest of adsorption experiments.

Effect of pH

The pH value of solution, which affects surface charge of ion exchange resin as well as degree of ionization,³⁷ has a big impact on adsorption process. Therefore, the effect of pH on the sorption of $\text{Ag}(\text{CN})_2^-$ should be studied carefully. As mentioned above, the study on pH effect below pH 9.0 was not done because of generation of HCN and actual pH value of $\text{Ag}(\text{CN})_2^-$ lixivium.

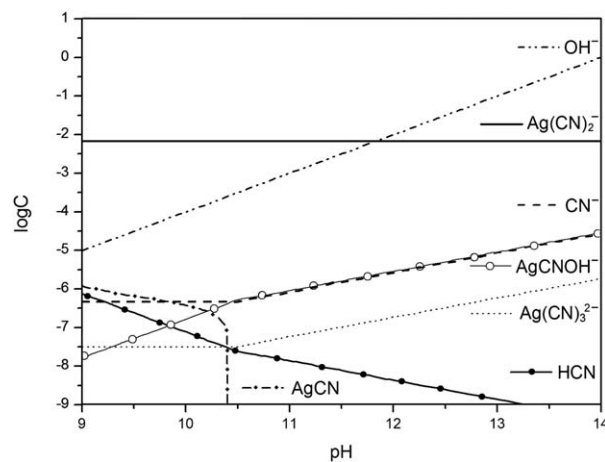


Figure 7. The speciation of $\text{Ag}(\text{CN})_2^-$ in solution with pH in the range of 9.0–14.0. $[\text{Ag}^+] = 6.68 \text{ mmol L}^{-1}$; $[\text{CN}^-] = 13.36 \text{ mmol L}^{-1}$.

The speciation of $\text{Ag}(\text{CN})_2^-$ in the range of 9.0–14.0 on the experimental concentration was shown in Figure 7. It was very helpful to understand the adsorption behavior. As shown in this scope, the concentration of $\text{Ag}(\text{CN})_2^-$ remained unchanged which was 6.68 mmol g^{-1} , whereas the concentration of other solutes, including OH^- , HCN, AgCN, CN^- , AgCNOH⁻, and $\text{Ag}(\text{CN})_3^{2-}$, changed with pH significantly. The maximum concentration of the species of silver-cyanide complex (HCN, AgCN, CN^- , AgCNOH⁻, and $\text{Ag}(\text{CN})_3^{2-}$ in the pH range of 9.0–14.0 was 7.84×10^{-4} , 1.12×10^{-3} , 2.68×10^{-2} , 2.81×10^{-2} , and $1.83 \times 10^{-3} \text{ mmol g}^{-1}$, respectively.

The effect of pH on the sorption of $\text{Ag}(\text{CN})_2^-$ onto cellulose 2 and cellulose 3 was shown in Figure 8. Cellulose 2 is a kind of weak base anion exchange resin, which contains abundant primary and second amine function groups, so it can absorb anions as well. However, as shown in Figure 8, the adsorption capacity of cellulose 2 was much lower than that of cellulose 3 in the given range of pH. The reason for this phenomenon can be ascribed to the protonation of amine groups of cellulose 2. Most weak base resins have a $\text{p}K_a$ of 6.0–8.0, therefore, only a small percentage of amine groups in cellulose 2 can convert into activated sites by the protonation when $\text{pH} > 7$.¹¹ Therefore, in the pH range of 9.0–14.0 very low exchange of metal-cyanide complex ion occurs in weak base anion exchange resin.¹⁸

In contrast, the charges of cellulose 3 are not pH-dependent, they come from positively charged nitrogen atoms joined by single bonds to methyl groups as shown in Figure 2, i.e., the

Table III. Comparison of Adsorption Time for Metal-Cyanide Complexes on Different Adsorbents

Adsorbent	Adsorbate	Adsorption time (h)	References
Purolite A500/2788 resin	Copper-cyanide complex	4	34
Kuraray QA6/12HAH	Copper-cyanide complex	>24	34
Lewatit MP-500	Copper-cyanide complex	1	34
Dowex 21K XLT resin	Gold-cyanide complex	1	3
Cellulose 3	Silver-cyanide complex	0.33	In this study

cellulose 3 possesses a permanent positive charge.¹⁸ Therefore, the quantity of $\text{Ag}(\text{CN})_2^-$ adsorbed on cellulose 3 mainly depended on the speciation of silver-cyanide complexes and emergence of competitive anions when the value of pH changed. As seen in Figure 8, the adsorption capacity of cellulose 3 declined slightly from 9.0 to 12.0, which was less than 9.5%. This result indicated that the cellulose 3 has a potential to be used in dealing with effluent of cyanidation. Because the concentration of the species of silver-cyanide complex is much lower than that of $\text{Ag}(\text{CN})_2^-$ in the given pH range as mentioned above. It is reasonable to regard the emergence of competitive anion, which is mainly the OH^- , as the main factor for the decline. Therefore, the modest decline might be explained mostly by the competition of OH^- with $\text{Ag}(\text{CN})_2^-$ for the sorption sites, because more and more OH^- ions were present in the solution with the increase of pH value.^{38,39} Especially after the pH value of 12, the number of OH^- ions considerably exceeded the number of $\text{Ag}(\text{CN})_2^-$ ions, as a result, more apparent fall was observed when pH changed from 12.0 to 14.0, which was nearly 60%.

Adsorption Isotherms

The analysis of experimental equilibrium data by fitting them into different isotherm models is an important step to propose suitable model for process design. As the isotherm indicates the adsorption capacity of the sorbent and enables the evaluation of adsorption performance, the involved mechanisms and parameters to be improved, which are of critical importance in optimizing the use of adsorbent. The most widely applied isotherms for data modeling are the Langmuir and Freundlich, which are developed based on thermodynamic equilibrium.^{18,23}

$$\text{Langmuir isotherm: } q_e = \frac{q_m b C_e}{1 + b C_e} \quad (5)$$

$$\text{Freundlich isotherm: } q_e = K_F C_e^{1/n} \quad (6)$$

where q_e is the amount of $\text{Ag}(\text{CN})_2^-$ in the resin (mmol g^{-1}); C_e is the equilibrium concentration (mmol L^{-1}); b is the Lang-

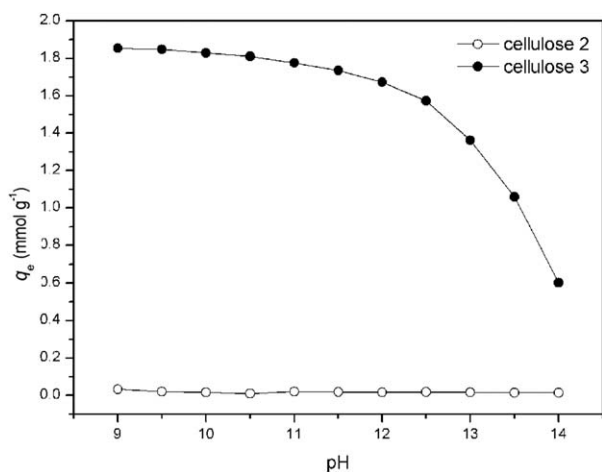


Figure 8. Effect of pH on the adsorption of $\text{Ag}(\text{CN})_2^-$ onto cellulose 2 and cellulose 3. $[\text{Ag}(\text{CN})_2^-] = 6.68 \text{ mmol L}^{-1}$; Adsorption time = 20 min; temperature = 25°C ; amount of adsorbent = 20 mg; stirring rate = 200 rpm.

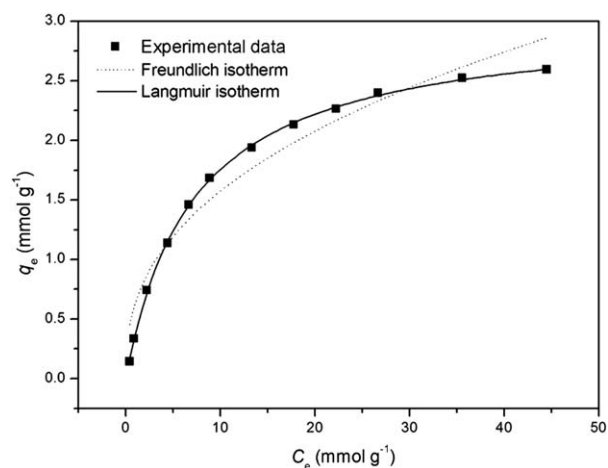


Figure 9. Comparison of the experimental and fitted isotherm curves for the adsorption of $\text{Ag}(\text{CN})_2^-$ onto cellulose 3. Adsorption time = 20 min; temperature = 25°C ; pH = 11.0; amount of adsorbent = 20 mg; stirring rate = 200 rpm.

muir isotherm constant (L mmol^{-1}) related to the affinity of binding sites; K_F is the characteristic constant related to the adsorption capacity (L g^{-1}); n is the adsorption intensity; q_m is the maximum monolayer coverage capacity (mmol g^{-1}).

Figure 9 showed the fitted curves based on Langmuir and Freundlich isotherm models. The estimated parameters were given in Table IV. As shown, the values of R^2 (correlation coefficient) of Langmuir isotherm model was higher than that of Freundlich isotherm model, and the much larger F value of Langmuir isotherm indicated it has more validity in fitting the experimental data. Furthermore, there was no big deviation between equilibrium adsorption capacity (q_m , $3.016 \text{ mmol g}^{-1}$) of Langmuir isotherm model and the concentration of active sites ($C_{-\text{NH}_3}^+$, $2.899 \text{ mmol g}^{-1}$). Considering these results, it can be said that Langmuir isotherm model a good correlation for adsorption of $\text{Ag}(\text{CN})_2^-$ on cellulose 3 in contrast to Freundlich isotherm model. Therefore, as the Langmuir isotherm model represents, the adsorption of $\text{Ag}(\text{CN})_2^-$ onto the surface of cellulose 3 can be regarded as monolayer sorption with finite number of identical sites.⁴⁰

The validity of cellulose 3 for $\text{Ag}(\text{CN})_2^-$ adsorption was justified by comparing its adsorption data with those presented in the literature. It has been found that the q_m in this study was higher than those obtained from nature or other synthesized adsorbents as shown in Table V. This comparison shows that cellulose 3 is effective for $\text{Ag}(\text{CN})_2^-$ adsorption.

The essential feature of the Langmuir adsorption can be expressed by means of R_L ,^{42,43} a dimensionless constant reported as a separation factor of equilibrium parameter for the prediction whether the adsorption system is favorable or not. R_L can be calculated using eq. (7).

$$R_L = \frac{1}{1 + b C_0} \quad (7)$$

where C_0 is the initial concentration of $\text{Ag}(\text{CN})_2^-$ solution (mmol L^{-1}).

Table IV. Values of Freundlich and Langmuir Constants for the Sorption of $\text{Ag}(\text{CN})_2^-$ onto Cellulose 3

<i>n</i>	Freundlich			Langmuir			
	K_F (L g^{-1})	R^2	<i>F</i> value	q_m (mmol g^{-1})	b (L mmol^{-1})	R^2	<i>F</i> value
2.497	0.6257	0.9488	521.49	3.016	0.139	0.9994	46,495.36

Table V. Comparison of q_m for Heavy Metal Complexes on Different Adsorbents

Adsorbent	Adsorbate	q_m (mmol g^{-1})	References
Purolite A500/2788	Copper-cyanide complex	1.20	34
Lewatit MP500	Copper-cyanide complex	0.402	10
Lewatit MP64	Copper-cyanide complex	0.116	10
Purolite A-500	Gold-cyanide complex	0.749	41
Bonlite BA304	Gold-cyanide complex	0.626	41
Dowex 21K XLT	Gold-cyanide complex	0.162	3
LK-4	Silver-thiocyanate complex	0.064	19
AV-17-10P	Silver-thiocyanate complex	0.015	19
Cellulose 3	Silver-cyanide complex	3.016	In this study

As the value of b was positive, the value of R_L was smaller than 1 in all the concentration range, indicating the adsorption of $\text{Ag}(\text{CN})_2^-$ on cellulose 3 was a favorable one. And the adsorption of $\text{Ag}(\text{CN})_2^-$ was more favorable at higher initial concentration than lower one.

Kinetics Study

The kinetic of adsorption is helpful to describe the mechanism of adsorption, which relates with the potential rate-controlling step and the adsorption process. In general, the kinetic behavior of most solid adsorption can be interpreted by pseudo-first-order and pseudo-second-order equations.^{44,45} The nonlinear form of the two kinetic models was shown as follows:

$$\text{Pseudo-first-order model: } q_t = q_e(1 - \exp^{-k_1 t}) \quad (8)$$

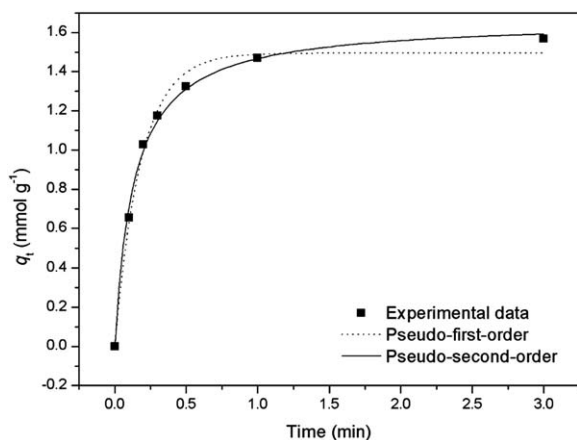


Figure 10. Comparison of the experimental and fitted kinetic curves by nonlinear method for the sorption of $\text{Ag}(\text{CN})_2^-$ onto cellulose 3. $[\text{Ag}(\text{CN})_2^-] = 6.68 \text{ mmol L}^{-1}$; adsorption time = 20 min; temperature = 25°C; pH = 11.0; amount of adsorbent = 20 mg; stirring rate = 200 rpm.

$$\text{Pseudo-second-order model: } q_t = \frac{k_2 q_e^2 t}{1 + k_2 q_e t} \quad (9)$$

which can be linearized as:

$$\text{Pseudo-first-order model: } \log(q_e - q_t) = \log q_e - \frac{k_1}{2.303} t \quad (10)$$

$$\text{Pseudo-second-order model: } \frac{t}{q_t} = \frac{1}{k_2 q_e^2} + \frac{1}{q_e} t \quad (11)$$

where q_e and q_t are the amounts of $\text{Ag}(\text{CN})_2^-$ adsorbed (mmol g^{-1}) at equilibrium and time t (min), respectively. k_1 (L min^{-1}) and k_2 ($\text{g}(\text{mmol min})^{-1}$) are the rate constants of first-order and second-order adsorption, respectively.

As can be seen in Figure 6, the whole process of adsorption could be completed in two phases, the initial rapid adsorption

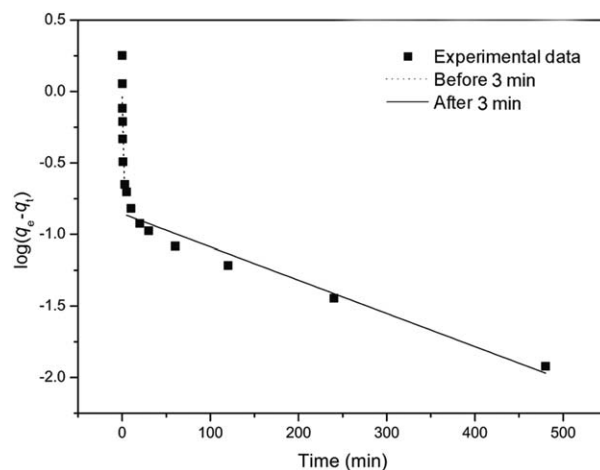


Figure 11. Comparison of the experimental and fitted kinetics curves by linear method for the sorption of $\text{Ag}(\text{CN})_2^-$ onto cellulose 3. $[\text{Ag}(\text{CN})_2^-] = 6.68 \text{ mmol L}^{-1}$; adsorption time = 20 min; temperature = 25°C; pH = 11.0; amount of adsorbent = 20 mg; stirring rate = 200 rpm.

Table VI. Values of Pseudo-First and Pseudo-Second Order Constants for the Adsorption of $\text{Ag}(\text{CN})_2^-$ onto Cellulose 3

Form	Pseudo-first-order				Pseudo-second-order			
	k_1 (L min^{-1})	$q_{e1, \text{cal}}$ (mmol g^{-1})	R^2	F value	k_2 (g (mmol min)^{-1})	$q_{e2, \text{cal}}$ (mmol g^{-1})	R^2	F value
Nonlinear	5.4409	1.495	0.9909	1707.20	4.505	1.662	0.9962	4046.16

Table VII. Values of Linear Pseudo-First-Order Constants for the Adsorption of $\text{Ag}(\text{CN})_2^-$ onto Cellulose 3 Before and After 5 min

Pseudo-first-order	0-3 min		3-480 min	
	R^2	F value	R^2	F value
Linear	0.5932	9.75	0.9450	121.20

occurred within about 3 min and was followed by the slow adsorption process, and the two phases were carefully analyzed, respectively.⁴⁶

In the first phase, the experimental data were fitted with the two kinetic models equations, and the fitted curves of nonlinear and linear form were shown in Figures 10 and 11, respectively, the estimated parameters of nonlinear form were listed in Table VI.

As shown in Figure 10 and Table VI, both of the two kinetic equations showed a good fit to the experimental equilibrium data, therefore, both first- and second-order kinetic occurred in the first 3 min. The higher value of R^2 and F value, obtained from pseudo-second-order, indicated the $\text{Ag}(\text{CN})_2^-$ sorption onto the novel resin followed pseudo-second-order kinetic model more better in the first phase. Therefore, the adsorption process was inferred to be a chemical process rather than physical one during the first 3 min, because the pseudo-second-order model assumes the rate-limiting step of the adsorption process is chemical sorption involving share or exchange of electrons between the adsorbents and metal ions.⁴⁵ In consideration of the good fit of pseudo-first-order and rapid adsorption, the diffusion must have an impact on the sorption in this phase too, because the pseudo-first-order assumes the adsorption is controlled by diffusion.⁴⁷ And with the influence of chemical process decline, the diffusion might play a more important role.⁴⁸

In the second region (beyond 3 min), the reaction gradually became independent of the surface sites with the saturation of exchange sites, and might proceed through a slow process of rearrangement of the $\text{Ag}(\text{CN})_2^-$ ion which controlled by

diffusion.⁴⁸ This deduction could be proved by the porosity structure of the resin and Boyd's analysis which suggested the metal uptake by dry beads was controlled by diffusion.⁴⁷ This deduction was also supported by the good linearity of pseudo-first-order in the later phase as shown in Figure 11, and the estimated parameters of pseudo-first-order in the first 3 min and later phase were calculated by the linear regression method and listed in Table VII. Both the value of R^2 and F value suggested the pseudo-first-order model had played a much more important role in the adsorption process after 3 min than before.

In verification experiment, the value of adsorption capacity of $\text{Ag}(\text{CN})_2^-$ on the novel adsorbent was $1.779 \text{ mmol g}^{-1}$ ($q_{e, \text{exp}}$), which was not in very good agreement with the calculated value came from pseudo-second-order ($q_{e2, \text{cal}}$, $1.662 \text{ mmol g}^{-1}$). The reason why $q_{e, \text{exp}}$ was larger than $q_{e2, \text{cal}}$ might be explained by the occurrence of rearrangement of $\text{Ag}(\text{CN})_2^-$ ion. With the results of porosity structure of the resin, there might be a slow diffusion from surface film into the pores with the saturation of sorption sites on surface, which could make a contribution to the adsorption capacity.⁴⁹ This fact also proved the applicability of pseudo-first-order model in the latter period of adsorption.

Therefore, the diffusion was a fast step at initial period, the interaction between metal ions and binding sites of modified cellulose beads was the rate-limiting step.⁴⁵ As the available adsorbing sites on the surface became saturated, rearrangement of $\text{Ag}(\text{CN})_2^-$ ions might occur, such as the diffusion of $\text{Ag}(\text{CN})_2^-$ ions from surface film into the pores of the resin. These made the $\text{Ag}(\text{CN})_2^-$ adsorption severely limited by diffusion which was consistent with the principle of pseudo-first-order model.⁵⁰

In addition, the efficiency of the obtained resin was justified by comparing its adsorption data with those presented in the literatures.^{18,23,41} It has been found that the rate constant value (k_2) of $\text{Ag}(\text{CN})_2^-$ adsorption onto the resin performed in this study was much higher than many other adsorbents' reported before as shown in Table VIII. There are several factors affect the adsorption kinetic. Mainly kinetic depends on the speed of

Table VIII. Comparison of k_2 and b for Metal Ion Complexes on Different Adsorbents

Adsorbent	Adsorbate	k_2 (g (mmol min)^{-1})	b (L mmol^{-1})	References
QMSC	Chromium-oxide complex	7.2×10^{-2}	18.0	18
SBAE	Chromium-oxide complex	0.22	4.50	41
Bonlite BA304	Gold-chloride complex	0.67	0.77	23
Purolite A-500	Gold-chloride complex	0.78	0.69	41
Cellulose 3	Silver-cyanide complex	4.51	0.14	In this study

coupling reaction and accessibility of the active groups of the support to adsorbed molecules.⁵¹ As seen in Table VIII, the affinity of silver-cyanide complex for cellulose 3 (b) was relatively low when compared with some other metal complexes.^{18,23,52} Therefore, we believed the accessibility, which was contributed by the design of highly basic function groups and outstretched spacer arms, might be the reason for the high value of k_2 .⁶ Hence, the novel anion exchange resin can be considered to be a potential and valuable approach for recovery of $\text{Ag}(\text{CN})_2^-$.

CONCLUSION

In this study, cellulose was made into spherical by double emulsification method, and then the cellulose beads were grafted with quaternary ammonium groups in tentacle-type by three substitution reactions. The degree of each substitution reaction was characterized by concentration of epoxy, amine, and quaternary ammonium functions, which were 0.854 mmol g⁻¹, 2.125 mmol g⁻¹, and 2.899 mmol g⁻¹, respectively. The studies of OM and SEM showed the modified cellulose beads possess excellent spherical shape and micropores structure. The novel resin was then evaluated for the adsorption of $\text{Ag}(\text{CN})_2^-$ using batch adsorption experiments. The results indicated the resin has a great potential to be used in alkaline condition, and the adsorption capacity has a tendency to grow over time and $\text{Ag}(\text{CN})_2^-$ concentration, respectively. It also proved the resin can reach its equilibrium adsorption in 20 min at pH of 11.0. In addition, the adsorption process was better explained by the Langmuir isotherm model which indicated the adsorption was monolayer adsorption, and the maximum monolayer adsorption capacity of $\text{Ag}(\text{CN})_2^-$ on the resin was determined to be 3.016 mmol g⁻¹. Moreover, the adsorption kinetics was proved closely followed the pseudo-second-order model in initial time followed pseudo-first-order model in later period, which mean the sorption process was limited by chemical sorption at first and then the rate-limiting step changed to diffusion gradually. Furthermore, the adsorption rate was found to be 4.505 g (mmol min)⁻¹, and the designs of long-spacer arms and highly basic function groups might have a contribution to this high value. Given the good performance of $\text{Ag}(\text{CN})_2^-$ adsorption, the novel anion exchange resin may have a great potential to be applied in varied separation fields including adsorption of $\text{Ag}(\text{CN})_2^-$.

ACKNOWLEDGMENTS

This work was supported by Foundation of Sichuan University for Young Teacher and Natural Science foundation of China.

REFERENCES

1. Tsuchida, N.; Muir, D. *Metal. Trans. B* **1986**, *17*, 529.
2. Syed, S.; Suresha, S.; Sharma, L.; Syed, A. *Hydrometallurgy* **2002**, *63*, 277.
3. Ok, Y. S.; Jeon, C. *J. Ind. Eng. Chem.* **2013**, *20*, 1308.
4. Desai, J.; Ramakrishna, C. *J. Sci. Ind. Res.* **1998**, *57*, 441.
5. Zhang, H.; Ritchie, I. M.; La Brooy, S. R. *J. Electrochem. Soc.* **2001**, *148*, D146.
6. Anilyte, J.; Liesiene, J.; Niemeyer, B. *J. Chromatogr. B* **2006**, *831*, 24.
7. Harris, W.; Stahlbush, J.; Pike, W.; Stevens, R. *React. Polym.* **1992**, *17*, 21.
8. Dicinowski, G. W.; Gahan, L. R.; Lawson, P. J.; Rideout, J. A. *Hydrometallurgy* **2000**, *56*, 323.
9. Wan, R.; Miller, J. *Miner. Process. Extr. Metall. Rev.* **1990**, *6*, 143.
10. Bachiller, D.; Torre, M.; Rendueles, M.; Díaz, M. *Miner. Eng.* **2004**, *17*, 767.
11. Fleming, C.; Cromberge, G. J. S. *Afr. Inst. Min. Metall.* **1984**, *84*, 125.
12. Cortina, J. L.; Warshawsky, A.; Kahana, N.; Kampel, V.; Sampaio, C. H.; Kautzmann, R. M. *React. Funct. Polym.* **2003**, *54*, 25.
13. Hailey, P.; Sherrington, D. *React. Funct. Polym.* **2000**, *43*, 195.
14. Hsieh, J. S.; Yoo, S. *J. Appl. Polym. Sci.* **2010**, *117*, 1476.
15. Du, K.-F.; Yang, D.; Sun, Y. *J. Chromatogr. A* **2007**, *1163*, 212.
16. Nagase, K.; Kobayashi, J.; Kikuchi, A.; Akiyama, Y.; Kanazawa, H.; Okano, T. *Langmuir* **2008**, *24*, 511.
17. Jain, P.; Sun, L.; Dai, J.; Baker, G. L.; Bruening, M. L. *Bio-macromolecules* **2007**, *8*, 3102.
18. Gurgel, L. V. A.; Perin De Melo, J. C.; De Lena, J. C.; Gil, L. F. *Bioresour. Technol.* **2009**, *100*, 3214.
19. Kononova, O.; Kholmogorov, A.; Danilenko, N.; Goryaeva, N.; Shatnykh, K.; Kachin, S. *Hydrometallurgy* **2007**, *88*, 189.
20. Liu, M.; Deng, Y.; Zhan, H.; Zhang, X. *J. Appl. Polym. Sci.* **2002**, *84*, 478.
21. Chinese Standard, G. Determination of the Epoxy Value of Plasticizers; General Administration of Quality Supervision, Inspection and Quarantine of the People's Republic of China and Standardization Administration: Beijing, China, **2008**.
22. Karnitz, O., Jr.; Gurgel, L. V. A.; De Melo, J. C. P.; Botaro, V. R.; Melo, T. M. S.; De Freitas Gil, R. P.; Gil, L. F. *Bioresour. Technol.* **2007**, *98*, 1291.
23. Wójcik, G.; Neagu, V.; Bunia, I. *J. Hazard. Mater.* **2011**, *190*, 544.
24. Rosentreter, J. J.; Skogerboe, R. K. *Anal. Chem.* **1991**, *63*, 682.
25. Cerjan-Stefanović, Š.; Briški, F.; Kaštelan-Macan, M. *Fresen. J. Anal. Chem.* **1991**, *339*, 636.
26. Navarro, R. R.; Sumi, K.; Matsumura, M. *Water Res.* **1999**, *33*, 2037.
27. Tiainen, P.; Gustavsson, P.-E.; Ljunglöf, A.; Larsson, P.-O. *J. Chromatogr. A* **2007**, *1138*, 84.
28. Kim, J. Y.; Lee, J. K.; Lee, T. S.; Park, W. H. *Int. J. Biol. Macromol.* **2003**, *32*, 23.
29. Muntean, S. G.; Paska, O.; Coseri, S.; Simu, G. M.; Grad, M. E.; Ilia, G. *J. Appl. Polym. Sci.* **2013**, *127*, 4409.
30. Zhou, Y.; Jin, Q.; Zhu, T.; Akama, Y. *J. Hazard. Mater.* **2011**, *187*, 303.

31. Wang, X.-Y.; Du, Y.-M.; Sun, R.-C.; Liu, C.-F. *J. Inorg. Mater.* **2009**, *24*, 1236.
32. Jones, L. H.; Penneman, R. A. *J. Chem. Phys.* **1954**, *22*, 965.
33. Chadwick, B.; Frankiss, S. *J. Mol. Struct.* **1968**, *2*, 281.
34. Dai, X.; Breuer, P.; Jeffrey, M. *Hydrometallurgy* **2010**, *101*, 48.
35. Wu, P.; Zhang, Q.; Dai, Y.; Zhu, N.; Dang, Z.; Li, P.; Wu, J.; Wang, X. *Geoderma* **2011**, *164*, 215.
36. Gupta, V.; Gupta, B.; Rastogi, A.; Agarwal, S.; Nayak, A. *J. Hazard. Mater.* **2011**, *186*, 891.
37. Elliott, H.; Huang, C. *Water Res.* **1981**, *15*, 849.
38. Yusof, A. M.; Malek, N. A. N. N. *J. Hazard. Mater.* **2009**, *162*, 1019.
39. Li, Z. *J. Environ. Eng.* **2004**, *130*, 205.
40. Del Bubba, M.; Arias, C.; Brix, H. *Water Res.* **2003**, *37*, 3390.
41. Nguyen, N. V.; Jeong, J.; Jha, M. K.; Lee, J.-C.; Osseo-Asare, K. *Hydrometallurgy* **2010**, *105*, 161.
42. Mattson, J. A.; Mark, H. B.; Malbin, M. D.; Weber, W. J.; Crittenden, J. C. *J. Colloid Interface Sci.* **1969**, *31*, 116.
43. Batzias, F.; Sidiras, D.; Schroeder, E.; Weber, C. *Chem. Eng. J.* **2009**, *148*, 459.
44. Lagergren, S. Zur Theorie der Sogenannten Absorption gelöster Stoffe, Kungliga Svenska Vetenskapsakademiens. Handlingar. Microchemical Journal Environ. Sci. Technol. J. Colloid Interface Sci J. Colloid Interface Sci Environ. Sci. Technol. Rev. Soc. Quím. Perú, American Water Works Association Chem. Eng. J. **1898**, *4*, 1.
45. Ho, Y.-S.; McKay, G. *Process Biochem.* **1999**, *34*, 451.
46. Singh, J.; Huang, P.; Hammer, U.; Liaw, W. *Clays Clay Miner.* **1996**, *44*, 41.
47. Lagoa, R.; Rodrigues, J. *Biochem. Eng. J.* **2009**, *46*, 320.
48. Varshney, K.; Khan, A.; Gupta, U.; Maheshwari, S. *Colloids Surf. A* **1996**, *113*, 19.
49. Abdullah, M.; Chiang, L.; Nadeem, M. *Chem. Eng. J.* **2009**, *146*, 370.
50. Chen, Y. X.; Zhong, B. H.; Fang, W. M. *J. Appl. Polym. Sci.* **2012**, *124*, 5010.
51. Atia, A. A. *Hydrometallurgy* **2005**, *80*, 98.
52. Lukey, G.; Van Deventer, J.; Chowdhury, R.; Shallcross, D. *Miner. Eng.* **1999**, *12*, 769.